Theory of Adsorption Processes at Ring–Disk Electrodes. Application to the Adsorption of Copper(I) in 0.5 *M* Hydrochloric Acid on Platinum

Stanley Bruckenstein[1] and D. T. Napp

Contribution from the Department of Chemistry, University of Minnesota, Minneapolis, Minnesota 55455. *Received June 17, 1968*

Abstract: The theoretical background necessary for the application of the rotating ring–disk electrode to the study adsorption processes at solid electrodes is presented. A study was made of the Cu(I)–Cu(II) system in 0.5 *M* HCl at a platinum rotating ring–disk electrode. The shapes of the curves for the disk current and ring current *vs.* time and potential were in excellent agreement with the theoretical predictions. At 0.0 V, 0.15 mC/cm^2 of Cu(I) is adsorbed on platinum for Cu(I) concentrations ranging from 10^{-6} to 2×10^{-3} *M*.

The rotating ring–disk electrode (RRDE) is a unique tool for studying the adsorption of an electrochemically active species. Several experimental approaches are possible and all depend upon the quantitative detection of the species produced or consumed at the disk electrode by means of the ring electrode. As it has been shown elsewhere,[2] the current at a ring electrode is related to the flux of material being consumed or generated at the electrode and depends solely on the geometric parameters of the RRDE, provided no kinetic complications exist. A discussion of four methods which could be used for studying adsorption at the RRDE is presented in this paper. Also, experimental results obtained for the Cu(I)–Cu(II) system on platinum in 0.5*M* HCl are reported.

Theoretical

Method 1. The disk electrode of a RRDE is potentiostated at an initial potential, E_i, such that a species, A, present in solution is adsorbed on the disk electrode. After adsorption equilibrium is reached on the surface of the electrode, the potential of the electrode is changed using a linear potential sweep on the order of 10 V/min to a final potential, E_f, where species A undergoes a redox reaction to produce another species, B, which is partially or completely desorbed. Assuming that A is the reduced form, reactions 1–4 may occur individually, sequentially, or simultaneously at the disk

$$A_{ads} = B_{ads} + ne \quad (1)$$

$$A_{ads} = B_{soln} + ne \quad (2)$$

$$A_{soln} = B_{ads} + ne \quad (3)$$

$$A_{soln} = B_{soln} + ne \quad (4)$$

electrode. We shall represent any or all these possibilities by

$$A = B + ne \quad (5)$$

The amount of B_{soln} can be determined using the ring electrode by setting its potential such that

$$B + ne = A \quad (6)$$

occurs, and the current corresponds to the limiting convective diffusion current. As will be clear in the context of this paper, when reaction 6 occurs at the disk electrode, the reverse of reactions 1 to 4 may be implied.

The ring current for reaction 6, i_r, is related to that portion of the disk electrode current, i_d, which produces B_{soln} by the expression

$$i_d = \mathbf{N} i_r$$

where **N** is the collection efficiency.[2] Hence, the time integral of the ring current is directly related to the total amount of B_{soln} produced at the disk electrode.

This technique is not subject to uncertainties arising from the double-layer charging current which flows at the disk electrode when its potential is changed.[3]

The adsorption properties of both A and B determined the type of disk current *vs.* disk potential (i_d–E_d) and ring current *vs.* disk potential (i_r–E_d) curves which may be observed. Several limiting cases are discussed below.

In a solution containing only species A, Figure 1, curve A, represents the i_d–E_d curve for reaction 5, when no adsorption processes are occurring. Figure 1, curve B, represents the i_d–E_d curve for reaction 5 when substantial amounts of A are adsorbed. Both curves have been corrected for double-layer charging current—a process which, in some cases, is more easily said than done.

Figure 1 also contains the various i_r–E_d curves which should be observed, depending upon the details of the adsorption processes. Curve C represents the shape expected when there are no adsorption processes. Curve C would also be obtained if B and A were equally adsorbed. The shape of the i_d–E_d curve is needed to distinguish between this situation and the case where no adsorption of A and B is occurring. Curve D represents the situation when considerable amounts of A are initially adsorbed and A is more adsorbed than B. If B is more adsorbed than A, curve E would be observed.

A simple variation of this method involves generating the adsorbed species electrochemically; *i.e.*, A can be generated *via* reaction 6 from a solution containing only B. If E_r is set in the limiting current region for reaction 6, i_d–E_d and i_l–E_d curves similar to those in Figure 1 will be obtained, with one important difference. In

(1) To whom all correspondence should be addressed at the Department of Chemistry, State University of New York at Buffalo, Buffalo, N. Y. 14214.

(2) W. J. Albery and S. Bruckenstein, *Trans. Faraday Soc.*, **62**, 1920 (1966).

(3) D. T. Napp and S. Bruckenstein, *Anal. Chem.*, **40**, 1036 (1968).

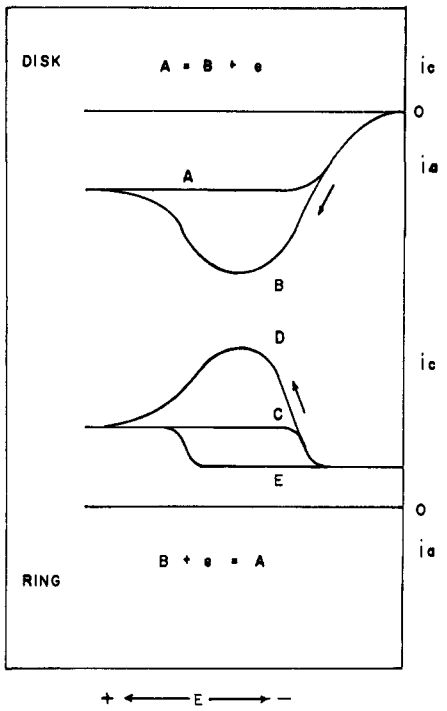

Figure 1. Idealized i_d–E_d and i_r–E_d curves in the presence of adsorption. Method I, voltage scan rate ~10 V/min from 0 V to more positive potentials: A, i_d–D_n curve, species A not adsorbed; B, i_d–E_d curve, species A adsorbed. Curves C, D, and E represent i_r–E_d curves: C, A not adsorbed or equal amounts of A and B are adsorbed; D, A more adsorbed than B; E, B more adsorbed than A. Rotation speed ~2500 rpm.

this case, the i_d–E_d curves will be displaced by a cathodic current corresponding to the limiting disk current for reaction 6. Similarly, the i_r–E_d curves will be displaced cathodically by a current equal to $\beta^{2/3}i_d$.[4-6] This method has been used elsewhere to establish the oxidation state of a copper species adsorbed on a platinum electrode in 0.5 *M* HCl[4] and in 0.2 *M* H_2SO_4.[7]

In method I, we have assumed that the rate of potential scan is sufficiently slow that steady-state convective diffusion equations describe the behavior of currents observed using the RRDE. Another group of methods are based on nonsteady currents which can be observed at the RRDE.

Method II. One nonsteady state approach makes use of the "transit time" of a species generated electrochemically at a disk electrode of a RRDE. Suppose a solution contains a species A of bulk concentration C_A^b greater than zero. The bulk concentration of its electrochemical oxidation product, B, is zero ($C_B^b = 0$). At the initial potential, E_i, of the disk electrode, E_d, species A is electrochemically inactive. The disk electrode potential is then stepped to a final potential, E_f, where A is electrochemically oxidized to B.

The potential of the ring electrode, E_r, is set such that all B reaching it will be reduced to A and thereby be detected by the appearance of a ring electrode current. Note that a time delay will occur after switching the disk electrode potential from E_i to E_f before any detectable amount of B will reach the ring electrode. The time, T, required for B generated at the outer edge of the disk electrode to reach the inner edge of the ring electrode is called the transit time.

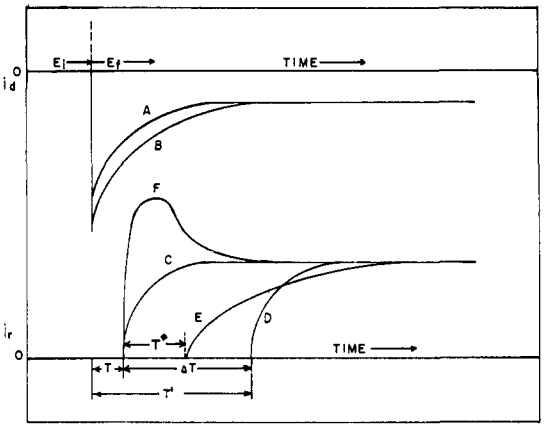

Figure 2. Idealized i_d–t and i_r–t curves obtained using method II: A, i_d–t curve, A not adsorbed; B, i_d–t curve, A adsorbed. Curves C, D, E, and F represent i_r–t curves; C, A, and B not (or equally) adsorbed; D, A not adsorbed, B rapidly and quantitatively adsorbed; E, A not adsorbed, partial and slow adsorption of B; F, A more adsorbed than B, and adsorption equilibrium is reached very rapidly.

It is convenient to express the experimental conditions in such RRDE experiments in a standard form. For the experiment described above, the conditions are $C_A^b > 0$, $C_B^b = 0$ for $t \geq 0$; $E_d = E_i$ at $t = 0$, no reaction, $i_D = 0$; $E_d = E_i$ at $t > 0$, A = B + ne, i_D = anodic; $E_r = E_i$ at $t = 0$, no reaction, $i_r = 0$; $E_r = E_i$ at $t > 0 + T$, B + ne = A, i_r = cathodic.

If B is not adsorbed at the disk electrode, B will immediately escape into the solution and will be transferred to the ring electrode by convective diffusion. In the latter case, Bruckenstein and Feldman derived the expression given by eq 7 for this transit time, T,[8] where

$$WT = 43.1(\nu/D)^{1/6}(\log R_2/R_1)^{2/3} \quad (7)$$

W = rotation speed in revolutions per minute and the other quantities have their previously defined electrochemical significance.[2]

If B is rapidly and quantitatively adsorbed, no B will escape the disk electrode surface until the electrode is saturated with B. Hence, detection of B at the ring electrode at time larger than T (eq 7) is *prima facie* evidence of adsorption of B.

Figure 2 contains current–time (i–t) curves for the ring (i_r–t) and disk (i_d–t) electrodes for some of the various adsorption situations which may arise in this method.

Curve A represents the i_d–t curve obtained at the disk electrode when A is not adsorbed. Curve B represents a curve which might be observed if A is adsorbed at E_i.

Curve C is the i_r–t curve which will be observed when neither A nor B is adsorbed, or when A and B are adsorbed equally. This case is described by eq 7.

Curve D should be observed when A is not adsorbed, while B is rapidly and quantitatively adsorbed. In this case, the transit time will be lengthened, and the difference between the transit time in the presence and

(4) S. Bruckenstein, *Electrokhimiya*, 9, 1085 (1966).
(5) W. J. Albery, S. Bruckenstein, and D. T. Napp, *Trans. Faraday Soc.*, 62, 1932 (1966).
(6) D. T. Napp, D. C. Johnson, and S. Bruckenstein, *Anal. Chem.*, 39, 481 (1967).
(7) G. W. Tindall and S. Bruckenstein, *ibid.*, 40, 1051 (1968).
(8) S. Bruckenstein and G. A. Feldman, *J. Electroanal. Chem.*, 9, 395 (1965).

absence of adsorption, ΔT, could be used to determine the amount of B adsorbed at the disk electrode by integrating the i_d–t curve from the time of switching the potential to a time equal in magnitude to ΔT.

Alternatively, the area between curves C and D can be determined. This area difference is proportional to the amount of B adsorbed at the disk electrode. Curve C can always be calculated from experimental data obtained using a solution containing a relatively high concentration of A. Under these circumstances adsorption effects are negligible compared to convective-diffusion phenomena.

Curve E should be obtained if A is not adsorbed while B is adsorbed on at least two kinds of electrode sites. The rapid and quantitative adsorption of B produces a zero value of i_r for $t^* \leq t - T$, while the rising ring current for $t > T^* + T$ results from the escape of some of the B generated at the disk electrode at times greater than T^*. The area difference between curve C and E is proportional to the amount of B adsorbed at the disk electrode.

Curve F would be obtained if A is adsorbed more strongly at E_i than B at E_f. The differences between curve C, in which there is no adsorption, and curve F, in which there is adsorption, is proportional to the difference between the amount of A which is adsorbed at E_i and the amount of B adsorbed at E_f.

Method III. A variation of method II involves the following experimental conditions. C^s represents the surface concentration of the subscripted species at the disk electrode. $C_A^b = 0$, $C_B^b > 0$ for $t \geq 0$; $E_d = E_i$ at $t = 0$, B + ne = A ($C_B^s = 0$), i_d = cathodic; $E_d = E_f$ at $t > 0$, A = B + ne, i_d = anodic until $t \sim T'$ ($C_B^s = 0$, $t \lesssim T' - T$); $E_r = E_i$ at $t = 0$, B + ne = A, i_r = cathodic; $E_r = E_i$ at $t > 0 + T'$, B + ne = A, i_r = more cathodic.

Depending upon whether or not A and B are adsorbed, different i_d–t and i_r–t curves may be observed, as shown in Figure 3.

Curve A is obtained if A is not adsorbed at the disk, while curve B results if it is adsorbed. The cathodic current when the potential of the disk is E_i corresponds to the convective-diffusion current for reaction 6. The i_r–t curve when $E_d = E_i$ and for short times after $E_d = E_f$ corresponds to $i_r = i_d(\beta^{2/3} - N)$.[4] At long times, the ring current is given by $i_r = i_d\beta^{2/3}$.[5] Curve C is obtained if A or B are not (or equally) adsorbed. Curve D is obtained when B is rapidly and quantitatively adsorbed, provided B is more adsorbed at E_f than A is at E_i. The area between curves C and D is proportional to the amount of B adsorbed at E_f in excess of the amount of A adsorbed at E_i.

Curves E and F correspond to the analogous situations described in connection with Figure 2.

The amount of B adsorbed (in excess of any A adsorbed) in curve D of Figure 3 can be calculated using steady-state ring–disk electrode theory. If the rate of adsorption of B is rapid and quantitative, the concentration of B in solution at the electrode surface remains zero after switching E_d from E_i to E_f until the disk electrode surface is saturated with B. During this process, the inward flux of B corresponds to the limiting convective-diffusion flux if we neglect the amount of B produced by the oxidation of A present in the diffusion layer. After the disk electrode surface is saturated with

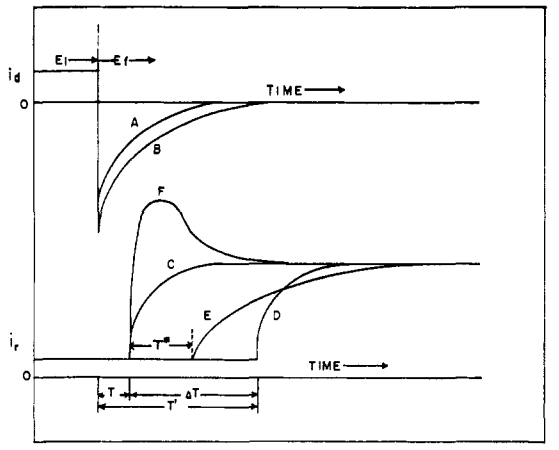

Figure 3. Idealized i_d–t and i_r–t curves obtained using method III: A, i_d–t curve, A not adsorbed; B, i_d–t curve, A adsorbed. Curves C, D, E, and F represent i_r–t curves: C, A, and B not (or equally) adsorbed; D, A not adsorbed, B rapidly and quantitatively adsorbed; E, A not adsorbed, partial and slow adsorption of B; F, A more adsorbed than B, and adsorption equilibrium is reached very rapidly.

B, B escapes into solution and is transferred to the ring electrode where it is detected amperometrically at the ring electrode, after a time, T'.

The observed transit time, T', is the sum of the ordinary transit time, T, when no adsorption occurs, plus the time, ΔT, required for adsorption of B supplied by convective diffusion of B present in the bulk of solution, *i.e.*

$$T' = T + \Delta T \tag{8}$$

The coulombs (Q_{ads}) of B adsorbed as a result of convective diffusion of B from the bulk of the solution is given by

$$Q_{ads} = i_d \Delta T \tag{9}$$

where

$$i_d = k_B W^{1/2} \tag{10}$$

and k_B is the proportionality constant in the Levich equation[9] taking into account the units of W. Note that this definition of i_d is exact, since a steady-state flux of B toward the electrode is established when the disk electrode is at E_i, and on switching the E_d to E_f, this steady-state situation is maintained as long as B is rapidly and quantitatively adsorbed at the disk electrode.

Combining eq 8, 9, and 10 yields

$$T' = T + Q_{ads}/k_B W^{1/2} \tag{11}$$

Equation 11 can be rearranged to eq 12

$$WT' = WT + \frac{Q_{ads}}{k_B} W^{1/2} \tag{12}$$

A plot of WT' *vs.* $W^{1/2}$ should yield a straight line with a slope equal to Q_{ads}/k_B, and intercept equal to WT. Note that WT is predicted by eq 7, and depends upon parameters which can be determined independently.

Method IV. It is not possible to use eq 12 of method III if A is more adsorbed than B. In such circum-

(9) V. G. Levich, "Physicochemical Hydrodynamics," Prentice-Hall, Englewood Cliffs, N. J., 1962, pp 63–69.

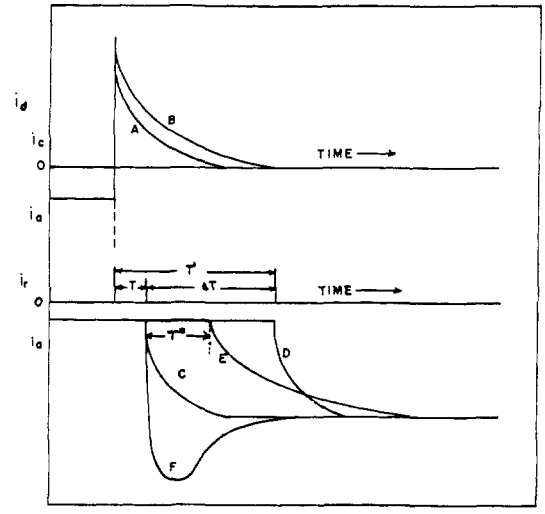

Figure 4. Idealized i_d–t and i_r–t curves obtained using method IV: A, i_d–t curve, A not adsorbed; B, i_d–t curve, A adsorbed. Curves C, D, E, and F represent i_r–t curves: C, A and B not (or equally) adsorbed; D, A not adsorbed, B rapidly and quantitatively adsorbed; E, A not adsorbed, partial and slow adsorption of B; F, A more adsorbed than B, and adsorption equilibrium is reached very rapidly.

stances, an experiment can be performed in a solution containing only A, *i.e.*, $C_A^b > 0$, $C_B^b = 0$ at $t \geq 0$; $E_d = E_i$ at $t = 0$, A = B + ne ($C_A^s = 0$), i_d = anodic; $E_d = E_f$ at $t > 0$, B + ne = A, i_d = cathodic until $t \approx T'$ ($C_A^s = 0$, $t \lesssim T' - T$); $E_r = E_i$ at $t = 0$, A_{soln} = B + ne, i_r = anodic; $E_r = E_i$ at $t > 0$, A_{soln} = B + ne, i_r = more anodic.

Initially, the disk electrode is held at a potential corresponding to the limiting current for the electrochemical oxidation of A to B, thereby maintaining the disk electrode surface concentration of A at zero. E_d is then stepped to a potential at which B is oxidized to A, and $C_B^s = 0$.

Figure 4 presents the various $i_d - t$ and $i_r - t$ curves which should be observed. The legend to Figure 4 specifies the various adsorption situations.

To a good approximation, eq 12 may be applied to experiments of the type represented by curves B and D. Equation 12 is not exact in this case because even though the concentration profile of A remains unchanged from $t = 0$ until the disk electrode surface is saturated with A, the concentration profile of B undergoes a change in the time immediately after the potential step as a result of the partial reduction of B in the diffusion layer to A_{ads}. So long as the amount of A_{ads} produced from B is small compared to that produced by steady-state convective diffusion, no serious errors will occur.

Methods I, II, and IV have been applied to the study of the adsorption of cupric and cuprous ions in 0.5 *M* HCl. The results of these studies are reported below.

Experimental Section

Chemicals. A stock 0.1000 *M* solution of cupric chloride was prepared by the method described by Bruckenstein and Prager.[10] This solution was diluted with water triply distilled from alkaline permanganate and with constant boiling hydrochloric acid to produce 10^{-3} *M* $CuCl_2$–0.5 *M* HCl and 2×10^{-3} *M* $CuCl_2$–0.5 *M* HCl solutions. The CuCl solutions were prepared by controlled potential electrolysis of the $CuCl_2$ solutions at −0.15 V using a large area platinum electrode. The $AgNO_3$–$HClO_4$ solution was prepared from Mallinckrodt Analytical Reagent 70% perchloric acid and Mallinckrodt Analytical Reagent silver nitrate crystals.

Equipment. The current–potential curves were recorded on two Houston Instruments HR T-2 x-y recorders. The current–time curves were recorded using either a Massa Meterite 260-A oscillographic recorder or a Tektronix 502 dual-beam oscilloscope.

A jacketed Pyrex glass cell which held 500 ml of solution was used as an electrolysis cell. Water was circulated through the jacket to maintain a constant temperature of 25 ± 0.5°. The solution was deaerated with repurified N_2.

The saturated calomel electrode (sce) was separated from the Luggin capillary containing the electrolysis solution by a closed ground-glass stopcock. All potentials were measured and recorded with respect to the sce. Potentials and currents were applied and measured at the ring–disk electrodes using a previously described electrochemical instrument.[6] The dimensions and geometric parameters of the RRDE used in this study are given below in Table I. Final polishing used 0.05-μ alumina on Buehler microcloth to produce a mirror finish. The electrodes were polished between experiments to remove any materials which remained as a result of previous electrochemical treatments. Before placing the electrode in the electrochemical cell, it was rotated at 900 rpm for 30 min at open circuit potential in 0.5 *M* HCl. The electrodes were rotated at speeds of 400–10,000 rpm, using an apparatus described elsewhere.[6]

Table I. Ring–Disk Electrode Parameters

Electrode	R_1,[a] cm	R_2,[b] cm	R_3,[c] cm	α[d]	β[e]	N[f]	S[g]
1	0.3874	0.3949	0.4045	0.059	0.087	0.121	0.36
2	0.3872	0.3971	0.4063	0.078	0.078	0.109	0.40

[a] Disk radius. [b] Inner ring radius. [c] Outer ring radius. [d] $\alpha = (R_2/R_1)^3 - 1$. [e] $\beta = (R_3/R_1)^3 - (R_2/R_1)^3$. [f] N = collection efficiency. [g] $S = 1 - (N/\beta^{2/3})$.

Uncompensated *IR* Drop. An uncompensated ohmic voltage drop is present in three electrode potentiostats because of the finite distance between the end of the Luggin capillary and the potentiostated electrode. A similar situation exists in the four electrode potentiostat used in this work. Generally, this *IR* drop is of no consequence if it can be kept sufficiently small. We measured the uncompensated resistance since its value was needed in an experiment reported below. First we sealed a platinum wire of the same dimensions as the Luggin capillary orifice, into a glass capillary, and cut the capillary at right angles to its axis. The cut end of the capillary was positioned in the same place as the Luggin capillary tip, and the resistance between the end of the wire and disk electrode measured when the electrochemical cell contained 0.5 *M* HCl. Replicate experiments using electrodes 1 and 2 gave resistances in the range 20–30 ohms.

Results and Discussion

Current–Potential Behavior of Cu(I) and Cu(II) in 0.5 *M* HCl. Figure 5 illustrates the i_d–E_d curves obtained for 10^{-3} *M* Cu(II) and for 10^{-3} *M* Cu(I) in 0.5 *M* HCl supporting electrolyte at a rotating platinum disk electrode. In the Cu(II) solution the first reduction wave corresponds to Cu(II) + e = Cu(I) while the second reduction wave corresponds to Cu(I) + e = Cu. In Cu(I) solution the anodic wave corresponds to Cu(I) = Cu(II) + e. Similar *i*–*E* curves are obtained at the platinum ring electrode of the RRDE.

Adsorption of Cu(I) on Platinum in 0.5 *M* HCl Using Method I. In connection with a study of electrochemical oxidation of platinum in 0.5 *M* HCl, method I was used to demonstrate that electrochemically generated Cu(I) is adsorbed on platinum.[3] Figure 12[3] has the form of the idealized case treated in this paper, Figure 1, since $C_{Cu(II)}^b = 10^{-6}$ *M*. The original purpose in ob-

(10) S. Bruckenstein and S. Prager, *Anal. Chem.*, 39, 1161 (1967).

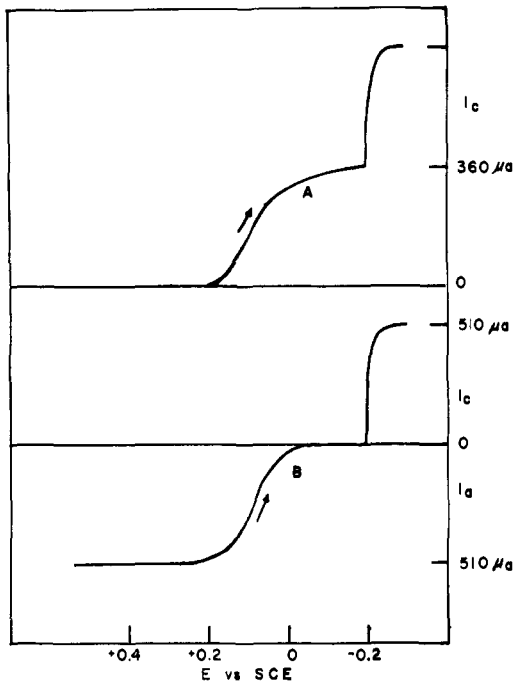

Figure 5. i_d–E_d curves for 10^{-3} M Cu(I) and 10^{-3} M Cu(II) in 0.5 M HCl; voltage scan rate = 200 mV/min, W = 2500 rpm; electrode no. 2; curve A, Cu(II); curve B, Cu(I)..

taining Figure 12[3] was to establish the oxidation state of the adsorbed copper species, and no attempt was made to determine the amount of adsorbed Cu(I). This experiment was repeated, and it was found that 0.15 mC/cm² of Cu(I) is adsorbed at 0.0 V.

Transit Time for a Nonadsorbed Species. The limiting convective-diffusion current for reaction 13 occurs

$$Ag(I) + e = Ag \qquad (13)$$

at a potential of +0.1 V in a 1 mM Ag(I)–0.1 M $HClO_4$ solution. In the same solution, at a potential of +0.5 V, no reaction is observed at a platinum electrode. Hence, when the potential of a disk electrode is stepped from +0.5 to +0.1 V, the flux of Ag(I) arriving at the ring electrode undergoes a sharp discontinuity at some time after the potential step has been applied to the disk electrode. This time should be equal to the transit time given by eq 7. Any adsorption of Ag(I) on platinum at +0.5 V cannot influence this experiment so long as the potentiostat is capable of supplying enough current to reduce any adsorbed Ag(I) in a time which is small compared to the transit time.

Table II. Nonsteady State Behavior of 9.9 × 10^{-4} M Silver in 0.1 M $HClO_4$

Electrode[a] rotation speed, rpm	Transit time, sec × 10^{-3}		WT, rpm sec[b]
400	40		16.0
900	18		16.2
1,600	10		16.0
2,500	7.0		17.5
3,600	5.0		18.0
4,900	4.0		19.6
6,400	3.0		19.2
8,100	2.0		16.2
10,000	1.8		18.0
		Av	17.5 ± 3.1

[a] RRPE no. 1. [b] WT (eq 7) = 15.0 (rpm sec).

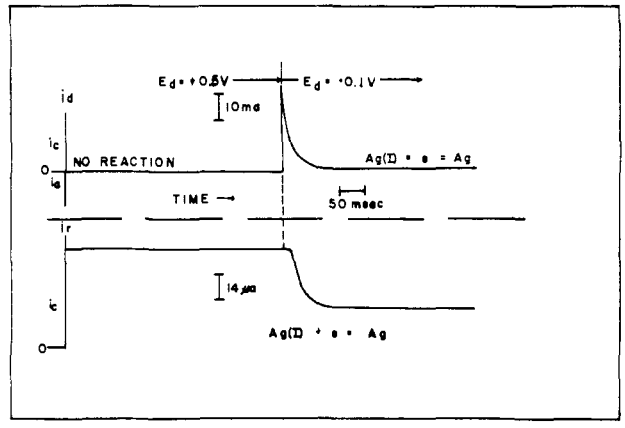

Figure 6. Transit time in the absence of adsorption: $C_{Ag(I)}{}^b$ = 9.9 × 10^{-4} M, C_{HClO_4} = 0.1 M; E_i(disk) = +0.50 V, E_i(disk) = +0.10 V, E_r = +0.10 V, W = 900 rpm; electrode no. 1.

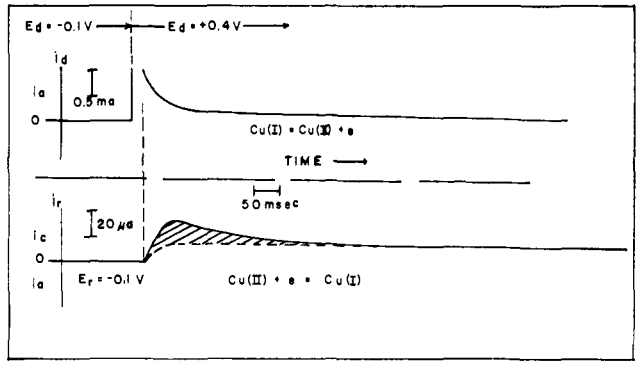

Figure 7. Application of method II to the adsorption of Cu(I) on platinum: $C_{Cu(I)}{}^b$ = 1.00 × 10^{-3} M, $C_{Cu(II)}{}^b$ = 0, C_{HCl} = 0.5 M, E_i(disk) = −0.1 V, E_i(disk) = +0.4 V, E_r = −0.1 V, W = 900 rpm; electrode no. 2.

A series of experiments were performed in a 9.9 × 10^{-4} M Ag(I)–0.1 M $HClO_4$ solution to test eq 7. A typical i_d–t and i_r–t curve is given in Figure 6 and a summary of the results obtained in Table II. Satisfactory agreement between theory and experiment is found.

Nonsteady State Adsorption Studies of Cu(I). A series of experiments was carried out in a 1 mM Cu(I)–0.5 M HCl solutions using the RRDE. The conditions for the first experiment, corresponding to method II, are given as follows: $C_{Cu(I)}{}^b$ = 1.00 × 10^{-3} M; $C_{Cu(II)}{}^b$ = 0; C_{HCl} = 0.5 M; E_d = −0.1 V, t = 0, no reaction; E_d = +0.4 V, $t > 0$, Cu(I) = Cu(II) + e; E_r = −0.1 V, t = 0, no reaction, $t > 0 + T'$, Cu(II) + e = Cu(I). Figure 7 gives typical i–t curves for the ring and disk electrodes obtained in such an experiment. These curves resemble the theoretical curves B and F of Figure 2. The product, WT = 16.9, indicates that Cu(II) is immediately desorbed from the ring electrode.

The shape of the i_r–i_t curve for $t > 0$ shows a maximum. We ascribe the shaded area between the solid and dotted i_r–t curves to Cu(II) produced from the oxidation of Cu(I) which was adsorbed on the disk electrode at −0.1 V; *i.e.*, the processes occurring at the disk electrode when E_d = +0.4 V are

$$Cu(I)_{ads} = (1 - x)Cu(II)_{ads} + xCu(II)_{soln} + e$$

$$Cu(I)_{soln} = Cu(II)_{soln} + e$$

where x represents the fraction of adsorbed Cu(I)

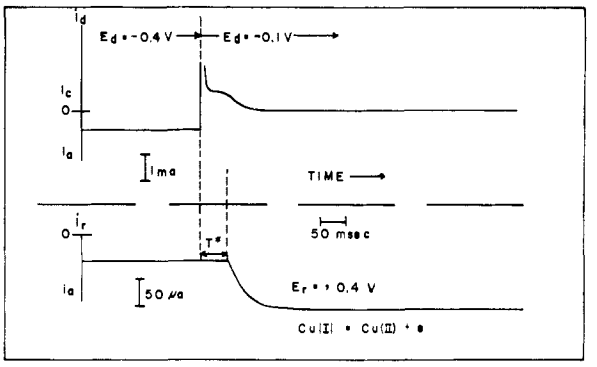

Figure 8. Applications of method IV to the adsorption of Cu(I) on platinum: $C_{Cu(I)}{}^b$ = 2.00 × 10^{-3} M, $C_{Cu(II)}{}^b$ = 0, C_{HCl} = 0.5 M; E_i(disk) = +0.4 V, E_f(disk) = −0.1 V, E_r = +0.4 V, W = 10,000 rpm, electrode no. 2.

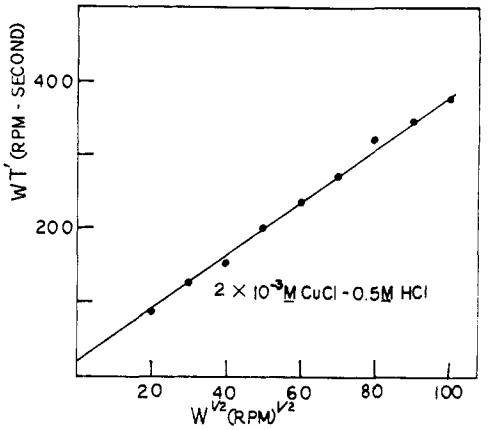

Figure 9. Test of eq 12. Data correspond to conditions in Figure 8, with W varying from 400 to 10,000 rpm.

which is oxidized to nonadsorbed Cu(II). We conclude from this experiment that if Cu(II) is adsorbed at a platinum electrode at a potential of +0.4 V, it is adsorbed to a lesser extent at 0.4 V than Cu(I) is adsorbed at −0.1 V. It would not be correct to conclude that Cu(II) is not adsorbed at +0.4 V since Cu(I) adsorbed at −0.1 V will be instantaneously oxidized to Cu(II) when the potential step is applied, thereby providing a source of Cu(II) in addition to that provided by the oxidation of convective-diffusion-supplied Cu(I).

Method II was applied to experiments analogous to that shown in Figure 7. The results of such experiments, as a function of rotation speed in the range 900–10,000 rpm, are shown in Table III. In this table, Q_r represents the shaded area, in microcoulombs, of Figure 7 for the specified rotation speeds. The last column, headed Q_r/N, corresponds to the amount of Cu(I) adsorbed per square centimeter at the disk electrode at −0.1 V in excess of the amount of Cu(II) adsorbed at +0.4 V, assuming the steady-state value of N may be used. The average value of Q_r/N = 0.15 ± 0.01 mC/cm².

Table III. Potential Step Data for 1.00 × 10^{-3} M Cu(I) in 0.5 M HCl

Rotation speed, rpm	Transit time,[a] sec	WT, rpm sec[b]	Q_r[c]	Q_r/N[d]
400	55	22.0	15.9	0.146
900	25	22.5	16.9	0.155
1,600	15	24.0	16.5	0.152
2,500	9.0	22.5	16.3	0.150
3,600	6.0	21.6	16.5	0.152
4,900	4.5	22.0	15.9	0.146
6,400	3.5	22.5	15.9	0.146
8,100	3.0	24.3	15.3	0.140
10,000	2.5	25.0	15.9	0.146
	Av	22.9 ± 2.1		

[a] RRDE no. 2. [b] WT (eq 7) = 22. [c] Charge in microcoulombs collected at the ring electrode divided by disk electrode area in square centimeters. [d] Previous column divided by collection efficiency; units are millicoulombs per square centimeter.

A potential step experiment was conducted in 2 × 10^{-3} M Cu(I) solution, for the conditions corresponding to method IV. The results of this experiment are given in Figure 8. In this experiment $C_{Cu(I)}{}^b$ = 2.00 × 10^{-3} M, $C_{Cu(II)}{}^b$ = 0, C_{HCl} = 0.5 M; E_d = +0.4 V at t = 0, Cu(I) = Cu(II) + e; E_d = −0.1 V at $t > 0$: (a) $Cu(II)_{diff\ lay}$ + e = $Cu(I)_{ads}$, (b) $Cu(II)_{ads}$ + e = $Cu(I)_{ads}$, (c) $Cu(I)_{soln} \rightarrow Cu(I)_{ads}$; E_r = +0.4 V at $t \geq 0$, $Cu(I)_{soln} \rightarrow$ Cu(II) + e.

At a disk electrode potential of +0.4 V, Cu(I) is oxidized to Cu(II) and the ring electrode current goes from $-i_d(\beta^{2/3} - N)$ at E_d = +0.4 V to $-i_d\beta^{2/3}$ as $t \rightarrow \infty$, when E_d = −0.1 V. After the potential of the disk electrode is stepped to −0.1 V, the three reactions labeled a, b, and c represent possible sources of copper(I) which can be adsorbed at the disk electrode. Reaction a is transient in nature and occurs as the result of Cu(II) which was produced in the diffusion layer while the disk electrode was at +0.40 V. Reaction b represents the reduction of adsorbed Cu(II) during the potential step, while reaction c represents the direct adsorption of copper(I) from solution. All of these reactions may be occurring simultaneously.

The i_d–t curve in Figure 8 supports the occurrence of reaction b. Lauer and Osteryoung[11] have observed a similar plateau in the i–t curves obtained in adsorption studies of Cu(II) at the hanging drop mercury electrode. They demonstrated that the size of the plateau observed in the i–t curve can be decreased by compensating for the ohmic voltage drop between the reference electrode and the indicator electrode. If a large amount of uncompensated resistance exists between these two electrodes, such a plateau will be observed, even if adsorption does not take place on the electrode surface. However, as was described in the Experimental Section, the uncompensated resistance is approximately 20–30 ohms; hence the i_d–t curve in Figure 8 demonstrates the reduction of adsorbed cupric ion. This conclusion is supported by the fact that the length of this plateau is independent of electrode rotation speed in the range 400–10,000 rpm.

Experiments corresponding to Figure 8 were performed at varying W and are present elsewhere.[12] WT varies sevenfold in going from 400 to 10,000 rpm and is always substantially larger than the value of 22 predicted by eq 7 for electrode 2. These data were plotted according to eq 12, and linear plots of WT' *vs.* $W^{1/2}$ were obtained. Figure 9 is the plot obtained for 2 × 10^{-3} M Cu(I). The intercept, 20, agrees well

(11) G. Lauer and R. A. Osteryoung, *Anal. Chem.*, 38, 1106 (1966).
(12) D. T. Napp, Ph.D. Thesis, University of Minnesota, 1967, Table IV, p 230.

with the predicted value of 22. From the slope we calculate that amount of Cu(I) absorbed on platinum at 0.1 V to be 0.158 mC/cm^2.

In an earlier study in 0.5 *M* HCl solutions known to contain 10^{-6} *M* Cu(I) or less, we found[3] that 0.15 mC/cm^2 of Cu(I) was adsorbed at platinum at 0.0 V. These experiments were performed at a rotating platinum disk electrode using the chronopotentiometric and linear scan voltammetric techniques. The results obtained in this work in concentration range 10^{-4} to 10^{-3} *M* Cu(I) and Cu(II) yield the same value for the amount of adsorbed Cu(I). At millimolar levels of Cu(II), i_d–t curves (Figure 8) suggest the presence of adsorbed Cu(II).

All our results are in agreement with those of Bowles[13] who used a radioisotope technique to demonstrate the adsorption of a monolayer of some copper species at potentials more negative than 0.15 V.

(13) B. G. Bowles, *Electrochem. Acta*, 10, 731 (1965).

Conclusion

The excellent agreement between the theoretical i_d–t and i_r–t curves for an adsorbed species and the corresponding experimental curves obtained in Cu(I) and Cu(II) solutions in 0.5 *M* HCl suggests that the ring–disk electrode technique will prove to a very powerful and useful method to study adsorption processes at solid electrodes.

Acknowledgment. This work was supported by the University of Minnesota Space Sciences Center under a grant from NASA, and by the National Science Foundation.

Intermolecular Radical–Solvent Hyperfine Coupling in Fluorocarbons

Joseph A. Potenza and Edward H. Poindexter

Contribution from the Institute for Exploratory Research, U. S. Army Electronics Command, Fort Monmouth, New Jersey 07703.
Received May 25, 1968

Abstract: Experimental dynamic nuclear polarization measurements at 74 G for a large number of fluorocarbon solutions containing free radicals led to four empirical conclusions independent of the system chosen for study: (1) protons in C–H bonds exhibit no detectable contact coupling in any solution; (2) aliphatic fluorocarbons are less positively enhanced than aromatic fluorocarbons in similar solutions; (3) nmr enhancements for aromatic fluorocarbons generally increase with fluorination; and (4) sterically well-shielded radicals give rise to large negative enhancements whereas poorly shielded radicals yield large positive enhancements. These trends are interpreted in terms of differences in intermolecular hyperfine coupling and complexation tendencies based on LCAO–MO calculations for three generalized radical–solvent collision types. Plane–plane collisions between aromatics are shown to be most effective in producing spin density at solvent nuclei; edge-on π collisions are least effective for all types of molecules. In addition, we show that radical–solvent hyperfine couplings are of the order of 1 G for all systems. This leads to the conclusion that differences in solvent spin density of approximately 10^{-3} electrons can account for the entire range of contact coupling observed and demonstrates the usefulness of dynamic nuclear polarization for the study of weak intermolecular interactions.

Recent studies of dynamic nuclear polarization (Overhauser effect) in dilute organic free radical solutions led to a number of interesting conclusions. Ultimate nmr signal enhancements, obtained by pumping radical epr signals, were shown to be sensitive to the nature and detailed chemical environment[1,2] of the resonating nucleus. In particular, protons invariably gave rise to large negative enhancements independent of the free radical or proton-containing solvent used, while for fluorine nuclei in similar solutions a wide range of enhancements was observed. The degree of ^{19}F polarization was then related to steric shielding in the free radical and to molecular properties of the fluorocarbon solvents based on pure dipole–dipole interactions for protons and varying degrees of scalar interaction for fluorine.

Two mechanisms[2] were proposed to account for the different degrees of fluorine scalar coupling: exchange polarization, after the manner of intramolecular coupling on free radicals, and transient complex formation. Physically, both mechanisms should lead to variations in the intensity of scalar interaction and in the scalar correlation time. On the basis of multifield dynamic polarization measurements,[3] we have previously shown that independent fluorine dipolar and scalar correlation times are necessary to characterize radical–fluorocarbon systems and that a relationship exists between scalar correlation time and observed enhancement. The purpose of the present communication is to extend our low-field experimental results to enable us to understand better the degree to which radical and solvent affect enhancement and to offer a molecular orbital interpretation for dynamic nuclear polarization results based on explicit radical–solvent interactions.

(1) E. H. Poindexter, J. R. Stewart, and P. J. Caplan, *J. Chem. Phys.*, 47, 2862 (1967).

(2) J. R. Stewart, E. H. Poindexter, and J. A. Potenza, *J. Am. Chem. Soc.*, 89, 6017 (1967).

(3) E. H. Poindexter, J. A. Potenza, D. D. Thompson, N. van Nghia, and R. H. Webb, *Mol. Phys.*, 14, 385 (1968).